SVU-IJVS-8(3), 37-59 Print ISSN: 2535-1826 Online ISSN: 2535-1877

Research Article Open Access

Morphological descriptions of the lingual apparatus in the western cattle egret (*Bubulcus ibis*): Functional Adaptations to Feeding Behavior

Ghada G. Adly*[1], Salma A. Mohamed[1], Mohammed Abdelsabour-Khalaf[1] and Soha Soliman[2]

[1]*Department of Anatomy and Embryology, faculty of Veterinary Medicine, South Valley University, Qena, Egypt.*
[2]*Department of Histology, faculty of Veterinary Medicine, South Valley University, Qena, Egypt.*

* Corresponding author: Ghada G. Adly. ghada_gaber@vet.svu.edu.eg

https://doi.org/10.21608/svu.2025.401320.1406

Submit Date: 06/07/2025; Revise Dat: 27/08/2025; Accept Date: 30/08/2025

ABSTRACT

The present study investigates the gross anatomy and microscopic structures of the tongue and its associated structures in the western cattle egret with the help of stereomicroscopy, light microscopy and scanning electron microscopy (SEM). This work was performed on ten heads of healthy adult cattle egret. These birds were trapped from different fields in Qena Governorate. Grossly, the tongue was a narrow-elongated organ carrying a markedly pointed tip that did not extend to the anterior limit of the mouth cavity. The U-shaped papillary crest on the dorsum of the tongue was the demarcation between the lingual body and root, which was at the same level of the lingual frenulum. Thus, the anterior free part of the tongue represented the larger percentage of the length of the tongue. The SEM revealed that the dorsal lingual surface was corrugated and exhibited many longitudinal microridges, which were separated by longitudinal microgrooves. The dorsal surface of the lingual root contained numerous openings of the ducts of glands. Histologically, thick keratinized stratified squamous epithelium lined most of the dorsum of the tongue, except its caudal part was non-keratinized type with intraepithelial mucous glands. Conversely, the ventral lingual epithelium was non-keratinized, except at the rostral part of the tongue, it was highly keratinized. Characteristically, the entoglossal bone supporting the lingual apex bifurcated at the lingual body into two caudal processes that in turn fused again at the level of the lingual root forming a single unit. The lingual submucosa showed the intralingual parts of the extrinsic skeletal muscles of the tongue. The lingual salivary glands were two groups located lateral to the entoglossum and they occupied most of the lingual submucosa, especially at the base of the tongue. The cells of the glands reacted positively with PAS. Our conclusion highlighted that the tongue structures are uniquely adapted to their specific function in one of the most prevalent insect-eating bird species in Egypt.

Keywords: *Cattle egret, Entoglossum, Intralingual muscles, Salivary glands, Tongue*

INTRODUCTION

Cattle egret is a worldwide heron species, it is a species of Family *Ardeidae*, Order *Pelecaniformes.* The initial description was given by Carl Linnaeus in *Systema naturae* as *Ardea ibis* (Linnaeus, 1758). The name is updated according to Bonaparte (1855) to be called *Bubulcus ibis*, the genus *Bubulcus* is the Latin name for a herdsman and it is given to the species that is associated with cattle. As it was described by McAllan et al. (1988) cattle egret can be classified into two subspecies according to geographical location: the western cattle egret, *B. ibis*, and the eastern cattle egret, *B. coromandus*. The former occupies a wide range including Western Asia, Africa, Europe and the Americas, while the latter is restricted to Eastern and South Asia as well as Australasia. (Ahmed, 2011). In Egypt, it refers to the white egret that is commonly seen in fields, and it is known in Arabic as Abu Qerdan (Moussa, 2014). Cattle egrets may feed in shallow water; however, it is mainly found in fields and dry grassy habitats, which is a result of their greater dependence on terrestrial insects and worms in their diet rather than aquatic prey (McKilligan, 2005; Mullarney et al., 2001).

The avian tongue is essential for a variety of functions, including sucking, filtering, catching, and manipulating food to compensate for the absence of other structures in the oropharyngeal cavity, such as teeth (Erdoğan and Iwasaki, 2014). The lingual apparatus in birds includes variable structures, such as the salivary glands, bony skeleton, cartilages, as well as extrinsic lingual muscles, all of which help its function (Homberger and Meyers, 1989; Madkour, 2020).

The birds exhibit a variety in the shape of the tongue that corresponded to the shape of their lower beaks and the feeding patterns of each species (El-Badry, 2022; Mahdy, 2021; Abumandour et al., 2019). By light microscopy, the tongue of birds has no internal muscle system, and it is covered by stratified squamous epithelium (Nickel et al., 1977).

Many previous studies have examined the oropharynx, its components and the covering beak, revealing morphological differences among various avian species. In this study, we focus on the lingual apparatus of cattle egret (*Bubulcus ibis*), and aim to investigate the specific morphological characteristics of its structures in relation to its diet, enabling it to select, lubricate, and swallow food effectively.

MATERIALS AND METHODS

Birds' collection and preparation

We carried out this work depending on ten healthy adult cattle egrets (*Bubulcus ibis*) that were obtained from fields in Qena Governorate. The adult age of cattle egret was determined according to the morphological description by McKilligan (2005) that the adult age group have a yellow beak, while the juvenile birds have black beak. The birds collected in this study were not sexed. The birds were anesthetized using a 1:1 mixture of ketamine and xylazine (0.0044 cc/kg injected into the pectoral muscle), then euthanized and allowed to fully exsanguinate

(Madkour and Abdelsabour-Khalaf, 2022). The heads were then cut off. Thorough washing of heads of the birds was carried out then all heads were incised along the commissures of the mouth to expose the oropharyngeal cavity.

Gross and morphometrical analysis

Heads of five birds were used. After washing well in the running tap water, the samples were fixed in 10% formalin. Various gross morphological features were recorded for each bird separately, and the samples were photographed in situ using a digital camera (XCAM, ToupTek, Zhejiang, China) attached to the stereomicroscope (SZ61, Olympus, Tokyo, Japan). The morphometrical analysis was carried out using image analysis; the needed parts were photographed using a camera phone near a caliper to provide a standard scale for measurement. These photographs were used to perform the measurements with ImageJ software.

Scanning electron microscopical preparations

The tongues of two birds were used. The specimens were carefully washed in normal saline and 1% acetic acid, then fixed in 4% glutaraldehyde solution for 24 hours. They were subsequently post-fixed in 1% buffered osmium tetroxide and washed in 0.1 M phosphate buffer at pH 7.4. The fixed samples were dehydrated in ascending grades of ethanol, followed by critical point drying in liquid carbon dioxide. Finally, all specimens were mounted on aluminium stubs covered with carbon tabs, sputtered with gold and examined with a JEOL scanning electron microscope (JSM-5400). Samples processing and examination were done in the electron microscope unit of Assiut University.

Coloring of the scanning electron microscopy images

Some SEM images were processed with Photo Filter 7.2.1 to apply color differentiation between various structures. This technique was employed by several authors (Madkour et al., 2023; Madkour, 2024; Abdellatif et al., 2024).

Light microscopical preparations

Tissue samples of three birds were taken for the preparation of paraffin blocks that were needed for the histological examination. The specimens were washed very well then fixed in 10% neutral buffered formalin for 24 hours. The fixed samples were kept in formic acid for the process of decalcification, and the good decalcification of the bone and the cartilage of specimens was tested physically under finger touch following Soliman and Madkour (2017). After proper decalcification of all specimens, they were dehydrated in ascending grades of ethanol (70-100%) and cleared in xylene following this, they were embedded in paraffin wax through stages I, II, and III, ultimately resulting in the formation of paraplast blocks. Specimen sections (3-5 μm) were cut using the LEICA 2165 rotatory microtome (RM 20352035; Leica Microsystems, Wetzlar, Germany) and mounted on glass slides. The prepared tissue sections were deparaffinized in xylene and rehydrated in a descending graded

series of ethanol (70-100%) until reaching distilled water. Finally, the tissue sections were stained with Harris' Hematoxylin and Eosin (H&E) stain for general histological examinations. The sections were treated with Periodic Acid-Schiff (PAS) reagent to detect the neutral mucopolysaccharides of the glandular tissue. Masson's trichrome stain was used to differentiate between the collagen and muscular fibers. The stain techniques were adopted by Bancroft and Gamble (2002). The nomenclature used was adopted by Nomina Anatomica Avium (Baumel, 1993).

Ethical standards

All methods in the present study were performed according to the guidelines for the use and care of birds of the ethical committee of the faculty of Veterinary Medicine, SVU, Qena, Egypt.

RESULTS

Gross anatomical observations and morphometrical analysis

Narrow elongated tongue lied on the floor of the oropharyngeal cavity. The tongue resembled a dagger in its outline, featuring a distinct pointed tip (Fig. 1A, B). The free tip of the tongue was situated 24.8 ± 1.66 mm from the rostral end of the beak (Fig. 1B) (Table 1). It could be subdivided into three parts: apex, body (middle part), and root. The lingual frenulum, a thin fold of mucous membrane, extended from the oral floor to the ventral aspect of the tongue, stabilizing it (Fig. 1A). Consequently, the lingual apex and body represented the anterior free part of the tongue which extended from the tip to the level of the frenulum. The lingual root, the posterior fixed part, was demarcated from the body of the tongue by the presence of the papillary crest (Fig. 1A, C). Morphometrically, the tongue measured about 36.2±1.66 mm long, its free part represented 70.7% of the total length of the tongue, while its fixed part represented only 29.3% (Table 1).

The U-shaped papillary crest carried a transverse row of small median caudally directed lingual papillae in addition to two giant conical papillae with markedly pointed free ends, the giant papillae were the largest papillae located at the both ends of the papillary crest and formed boundaries of the anterior half of the lingual root (Fig. 1C). Of note, both the lingual frenulum and the transverse row of the lingual papillae were located in the same level (Fig. 1A). Dorsally, the tongue was crossed longitudinally by a median lingual groove (*Sulcus lingualis medianus*) (Fig. 1C). It measured 8.56±0.42 mm long, and began about 12.5±2.2 mm caudal to the anterior end of the tongue and continued caudally crossing the transverse row of the lingual papillae and split it into two symmetrical halves, each half had four small median papillae in addition to one giant papilla was situated laterally. The ventral surface of the tongue showed a median longitudinal ridge (Fig. 1D).

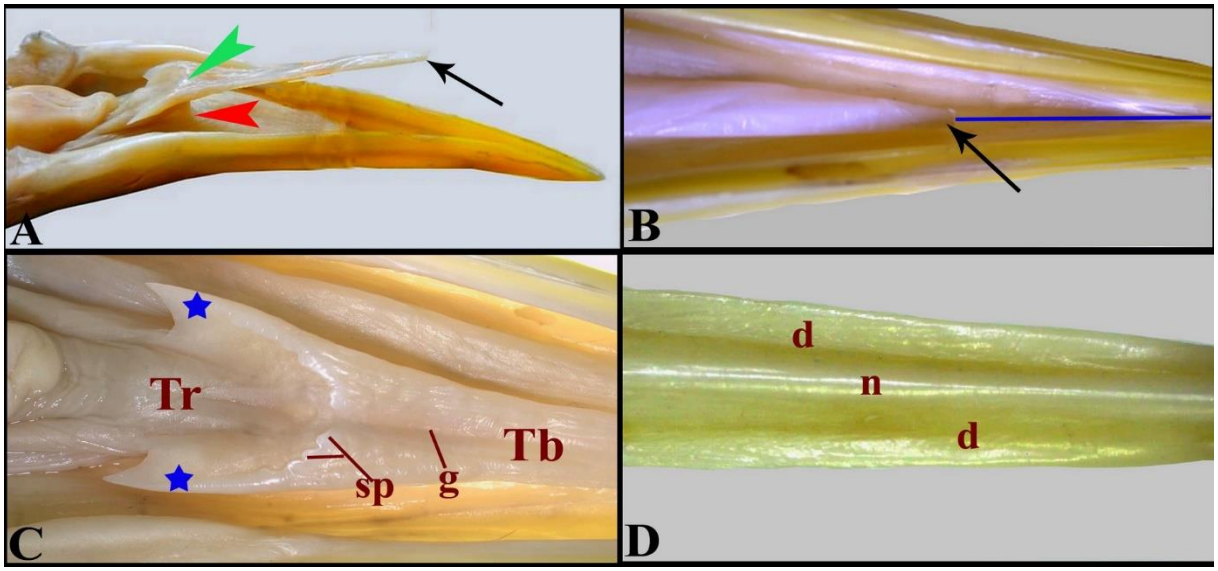

Figure (1): Gross photographs (A-D) showing the anatomical structure of the tongue in cattle egret. Note, anterior free tip (black arrow; A&B), lingual frenulum (red arrowhead; A), lingual papillary crest (green arrowhead; A), soft oral floor anterior to the tongue (blue line; B), lingual body (Tb; C), fixed part of tongue (Tr; C), dorsal lingual groove (g; C), small papillae of papillary crest (sp; C), two giant papillae (two blue stars; C), ventral longitudinal ridge (n; D), and flattened areas (d; D). B-D: photographs with the help of stereomicroscopy.

Table 1: Macro-morphometrical analyses of the tongue of cattle egret

Dimensions	Mean (mm)	SE
Length of:		
Tongue (total length).	36.2	1.66
Free part of tongue.	25.6	1.8
Fixed part of tongue.	10.6	0.68
Distance between lingual tip and tip of the beak.	24.8	1.66
Median lingual sulcus.	8.56	0.42
Lingual tip which was not crossed by lingual sulcus.	12.5	2.2
Ratio (%) of length of:		
Free part to total length of tongue.	70.7	
Fixed part to total length of tongue.	29.3	
Width of tongue at:		
Middle of its free part.	2	0.32
Level just rostral to frenulum linguae.	3	0.32
Middle of fixed part.	4.4	0.68
Number of lingual papillae at papillary crest:		
Total number.	10	
Giant papillae.	2	
Small median papillae	8	

Scanning electron microscopical examinations

The dorsal surface of the lingual apex and body showed scale-like structures covering the whole surface. These lingual scales were numerous at the level of the lingual body when compared with those on the lingual apex (Fig. 2C, D). Additionally, the dorsum of the tongue appeared uneven; it exhibited several longitudinal microgrooves that were marked by longitudinal microridges (Fig. 2E). As for the dorsal surface of the lingual root, it contained numerous openings of the ducts of the salivary glands (Fig. 3G). The surface two lateral extensions of the lingual root relating to the giant papillae was covered by a few lingual scales (Fig. 3F). Exceptionally, the lingual sulcus, only at the caudal part of the lingual body displayed a few openings of the ducts of the salivary glands (Fig. 3B, C). The midsagittal section at the level of the lingual body revealed that the lingual core consisted of an entoglossal bone as well as a skeletal muscle bundle ventral to it. Of note, the dorsal lingual surface was thinner than the ventral surface (Fig. 2F).

Histological examinations

By light microscope, the tongue of cattle egret was lined by stratified squamous epithelium that was composed of stratum basale, stratum spinosum and stratum corneum. The anterior lingual tip showed lamina epithelialis of nearly constant height, covering the whole tongue, which in turn was covered by a highly organized and thick keratin layer. The lingual core was represented by a highly vascularized dense, irregular collagenous connective tissue (Fig. 4A, B). Caudally, the keratin layer surrounding the tongue decreased in thickness, except ventrally at the level of the median longitudinal ridge, where it remained notably thick. The submucosa contained a rostral extension of a hyoid element, known as *the entoglossum*, which was made of hyaline cartilage. Chondrocytes were within the lacunae, and the cartilage was surrounded by perichondrium (Fig. 4C, D).

The dorsal aspect of the lingual body was covered by a thick keratinized stratified squamous epithelium that continued on the lateral edges of the tongue. In addition to the deep median longitudinal sulcus that crossed the dorsal surface of the tongue, there were three longitudinal microgrooves; one right and two left to the main lingual sulcus. At each side of each microgroove, there was a microridge (Fig. 5B, C). The serial sections revealed that these microgrooves appeared caudal to the beginning of the median lingual sulcus and extended to a distance backwards. On the other hand, non-keratinized epithelium lined the ventral surface and showed interdigitating folds of epithelium (epithelial pegs) with connective tissue papillae (Fig. 5D). At the caudal part of the lingual body, non-keratinized epithelium with intraepithelial mucous glands lined the ventral surface of the tongue (Fig. 6D).

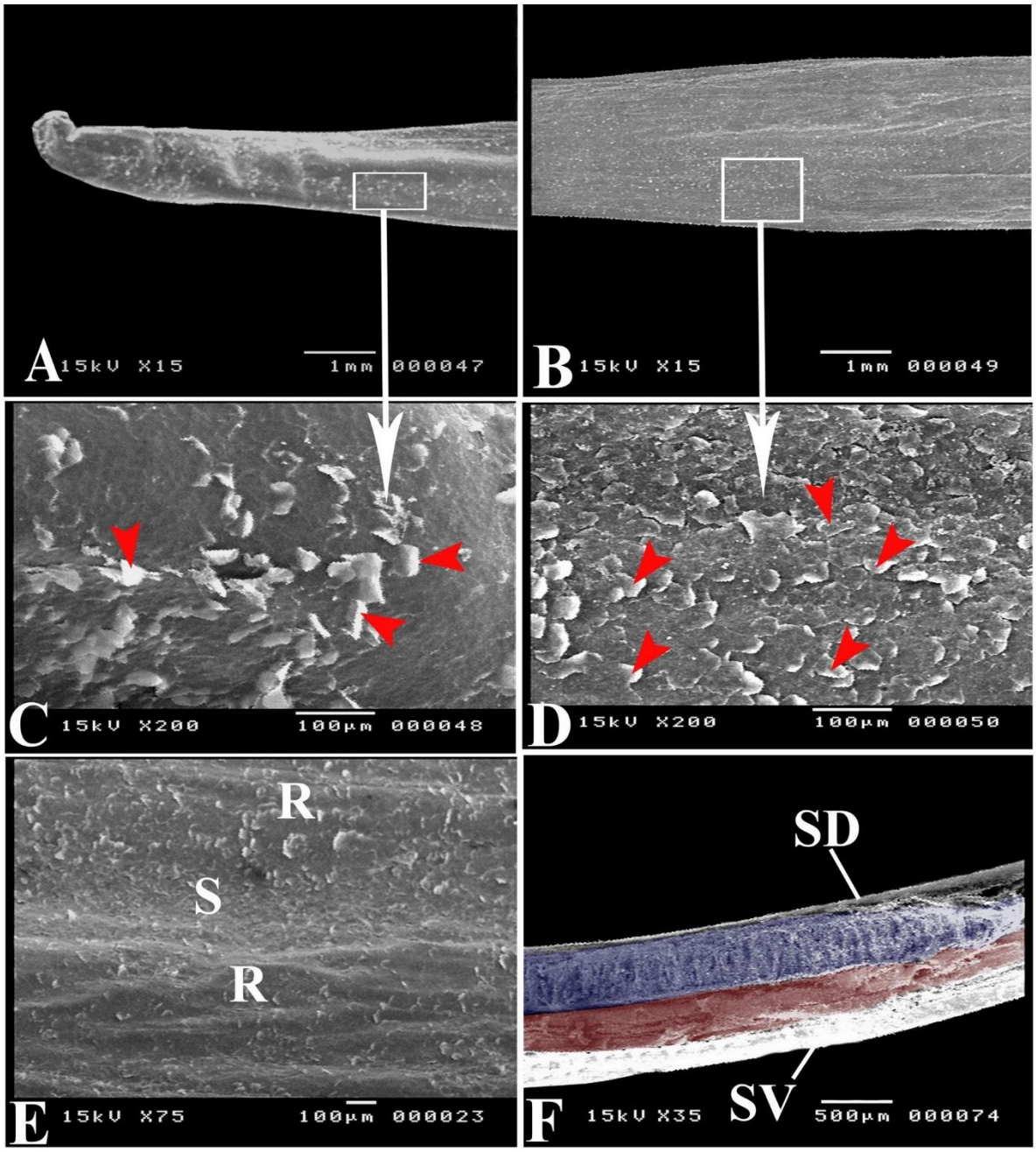

Figure (2): Photographs (A-E) showing the microscopic view of the dorsal surface of the lingual apex and the anterior part of the lingual body by SEM. Photograph (F) showing the microscopic view of a midsagittal section at the lingual body by SEM. Note, the lingual apex (photograph A), the lingual body (photograph B), scattered lingual scales (red arrowhead; C&D), microgroove (S; E) and microridges (R; E), dorsal surface (SD; F), ventral surface (SV; F), entoglossal bone (blue color; F), and skeletal muscle bundle (red color; F).

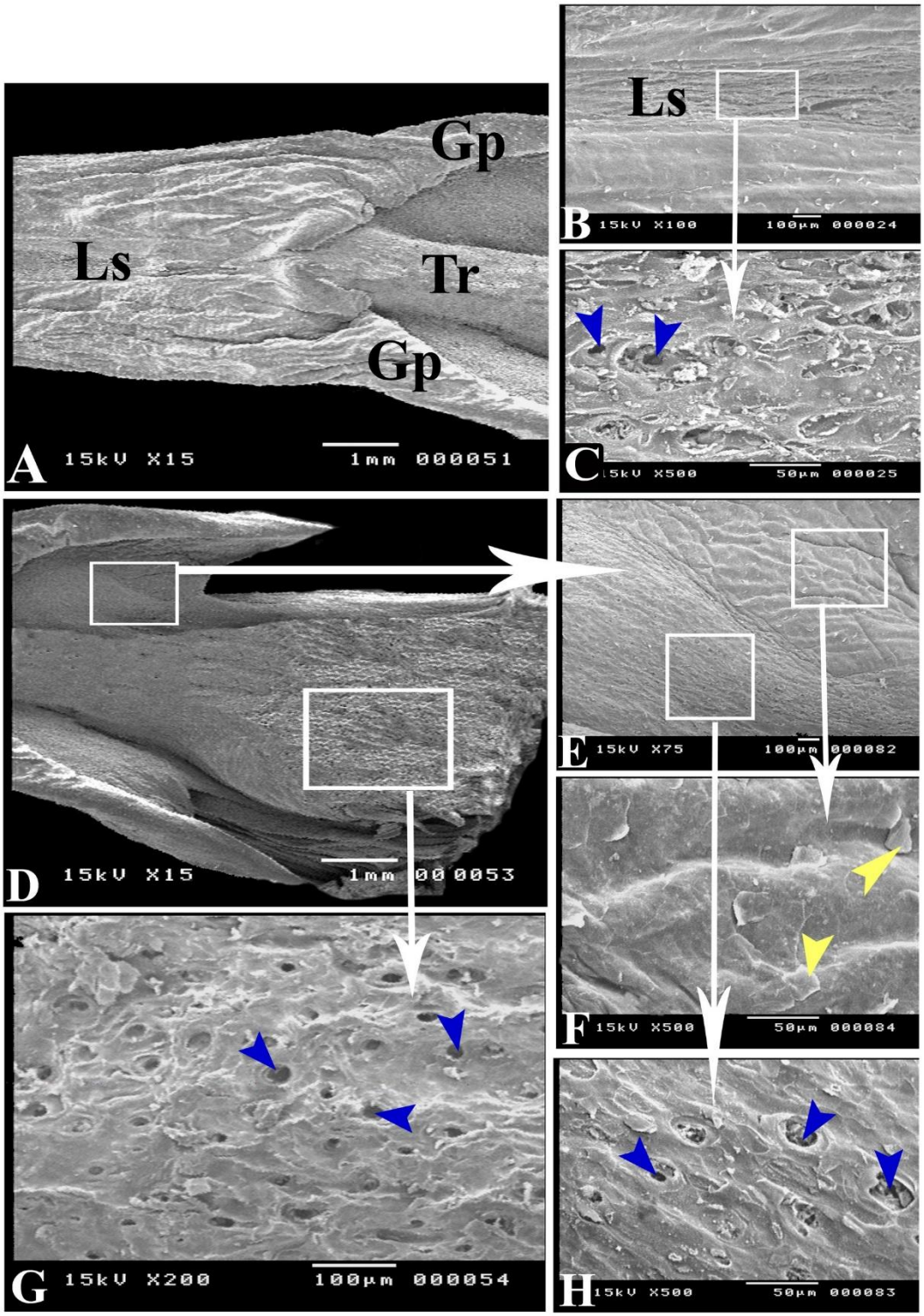

Figure (3): Photographs (A-H) showing the microscopic view of the dorsal surface of the posterior part of the lingual body and the lingual root by SEM. Note, lingual sulcus (Ls; A&B), giant papillae (Gp; A), lingual root (Tr; A), openings of glands (blue arrowheads; C, G&H) and desquamated epithelial cells (yellow arrowheads; F).

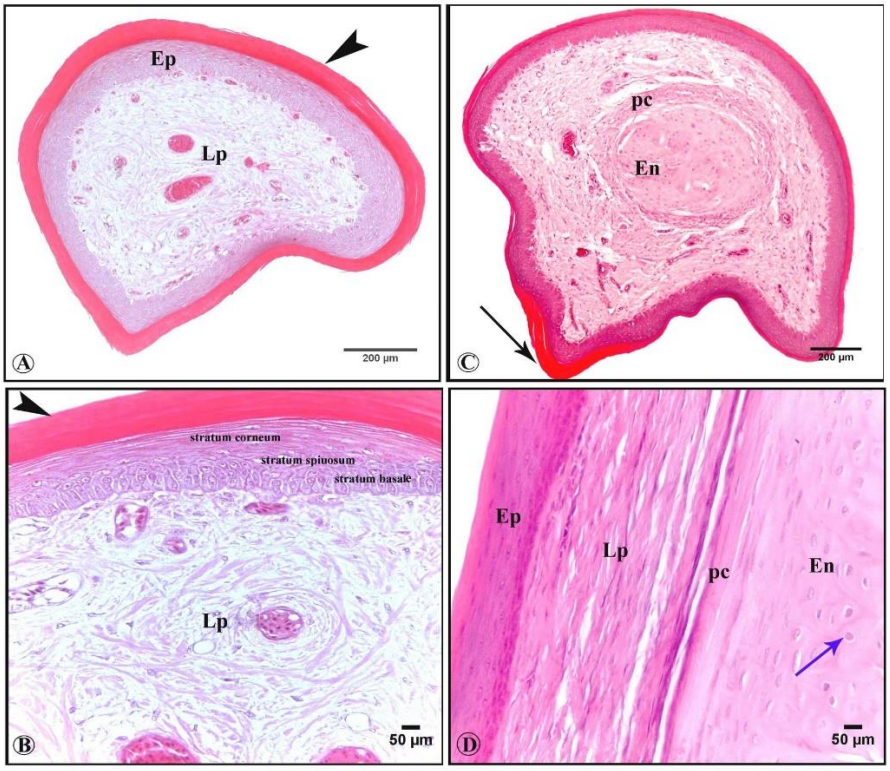

Figure (4): A: Photomicrograph at the most anterior part of the tongue of cattle egret shows stratified squamous epithelium (Ep) with a thick and highly organized keratin layer (black arrowhead). **B:** Magnified image shows the epithelium is formed of stratum basale, stratum spinosum and stratum corneum covering a core of vascular collagenous connective tissue (Lp). **C:** Caudal section at the anterior part of the tongue shows thick keratin layer covers the ventral median ridge (black arrow), a rostral extension of the entoglossum (En), which is surrounded by connective tissue (pc). **D:** Longitudinal section at the anterior part of tongue shows epithelium (Ep), lamina propria (Lp), entoglossum (En), with the chondrocytes are within the lacunae (blue arrow), and perichondrium (pc). All sections were stained with H&E stain.

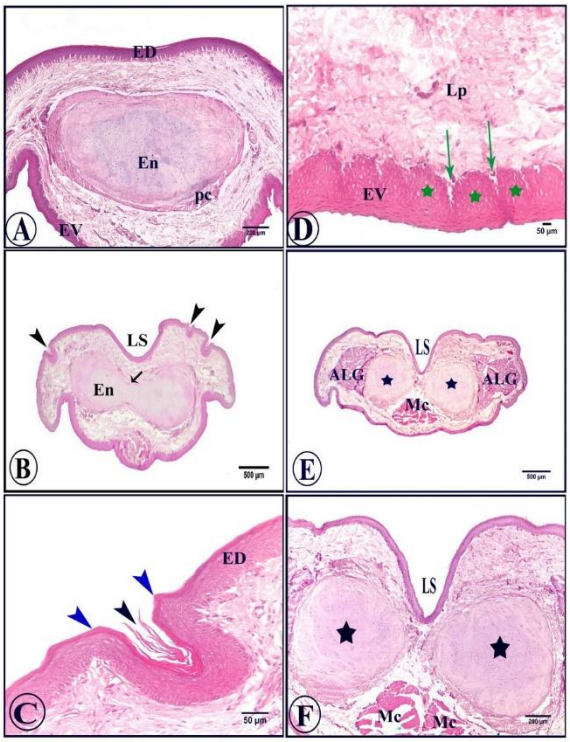

Figure (5): Histological images at the lingual body of cattle egret. **A:** Cross section at the anterior part of the lingual body shows dorsal epithelium (ED), ventral epithelium (EV), flattened entoglossum (En) and perichondrium (pc). **B:** Cross section at the middle part of the lingual body shows deep median longitudinal sulcus (LS), microgrooves (black arrowheads) and the entoglossum (En) begins to bifurcate (black arrow). **C:** Magnified image shows microgroove (black arrowhead) and two microridges (blue arrowheads). **D:** Magnified image shows non-cornified ventral epithelium (EV) with epithelial pegs (green stars) and connective tissue papillae (green arrows), and lamina propria (Lp). **E:** The entoglossum is divided into two caudal processes (two black stars), lateral to each process is a group of anterior lingual glands (ALG), ventromedially is the ceratoglossus muscle (Mc). **F:** Magnified image shows two caudal processes of entoglossum are cartilaginous (two black stars), ceratoglossus muscle is related to entoglossum (Mc). All sections were stained with H&E stain.

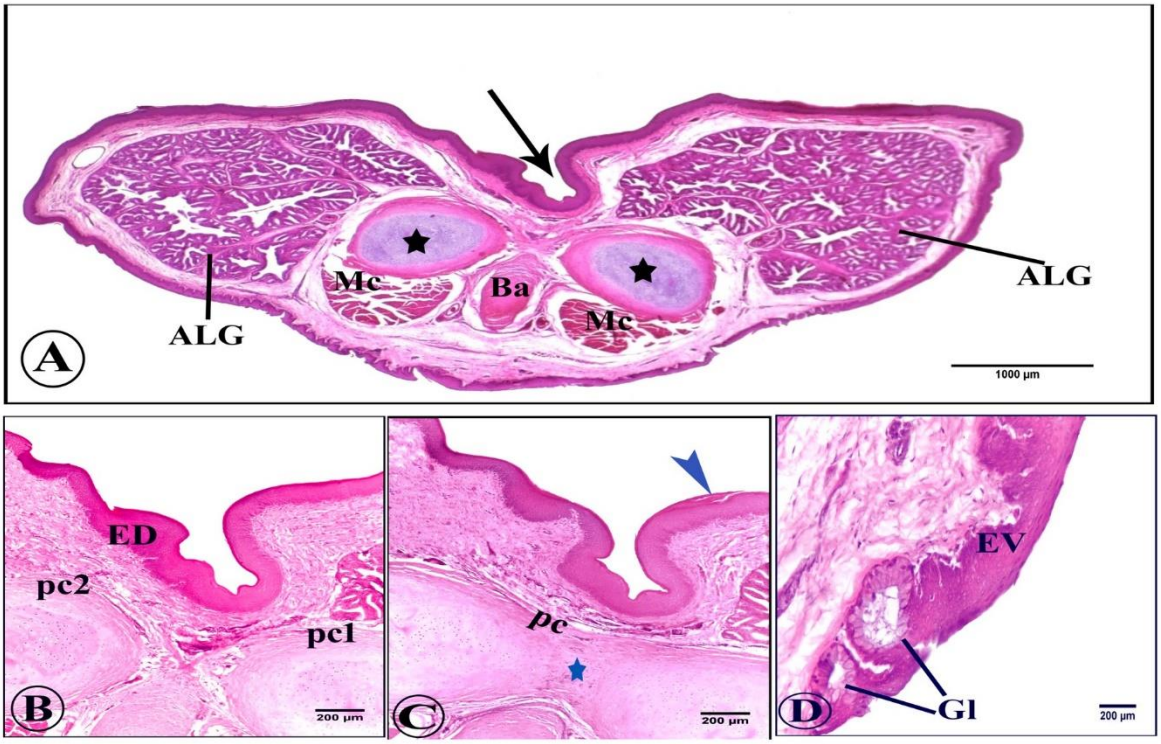

Figure (6): Histological images at the caudal part of the lingual body of cattle egret. **A:** Photomicrograph shows deep lingual sulcus (black arrow), laterally situated anterior lingual glands (ALG), two caudal processes of entoglossum (two black stars), the anterior process of basihyal (Ba), and the muscle ceratoglssus (Mc). **B:** Magnified image shows dorsal epithelium is keratinized type (ED), each caudal process of the entoglossum is surrounded by a perichondrium (pc1, pc2). **C:** Photomicrograph shows the union of the two caudal processes of entoglossum (blue star) with a single perichondrium (pc). Note, the keratin layer covers the dorsal epithelium (blue arrowhead). **D:** Magnified image shows ventral epithelium which is non-keratinized type (EV), with intraepithelial glands (Gl). All sections were stained with H&E stain.

At the papillary crest level, the lingual papillae were formed of connective tissue core and were covered by keratinized stratified squamous epithelium (Fig. 7A, B). The dorsal epithelium was non-keratinized stratified squamous epithelium showing interdigitating epithelial folds with connective tissue papillae. Close to the median plane of the tongue, the dorsal epithelium was non-keratinized with intraepithelial glands that reacted strongly positive with PAS technique (Fig. 7C, D). Ventrally, the surface epithelium showed spiny projections (Fig. 7E).

The dorsal surface of the lingual root was covered by non-keratinized epithelium with intraepithelial mucous glands (Fig. 8C). These glands gave strong positive results with PAS technique (Fig. 10F). The lingual papilla was covered by keratinized epithelium that continued on the lateral edges of the tongue (Fig. 8B). Ventrolaterally, the ducts of the posterior lingual glands opened (Fig. 8D). The lingual submucosa at the lingual body level showed the entoglossum that supported the tongue. The body of the entoglossal bone anteriorly was dorso-ventrally flattened (Fig. 5A). Backwardly,

the entoglossum was bifurcated into two parts: right and left caudal processes (Fig. 5E, F). Surprisingly, at the papillary crest level, the two caudal processes rejoined medially and were tied by means of syndesmosis, then fused again into a single unit (Fig. 7F), creating a circumscribed hole within the entoglossum. In the caudal lingual body, another hyoid skeletal element emerged (the basihyal, *os basibranchial rostralis*), extending rostrally as a rod-like process ventromedial to the entoglossum. The basihyal was cartilaginous at the lingual body level (Fig. 7A), but it ossified at the lingual root level (Fig. 8A).

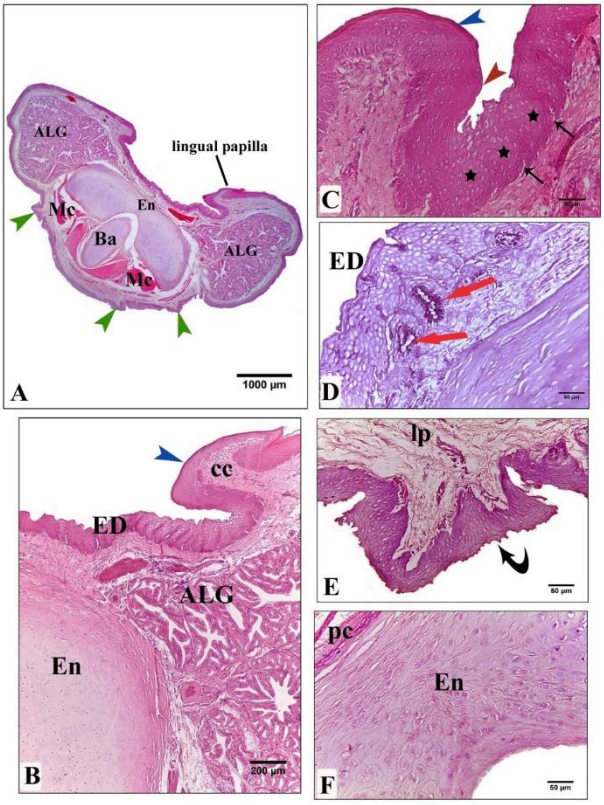

Figure (7): Histological images at the papillary crest level in cattle egret. **A:** Photomicrograph shows lingual papilla at the dorsum of the tongue, entoglossum (En), basihyal (Ba), muscle ceratoglossus (Mc), anterior lingual glands (ALG), and epithelial folds at the ventral surface of the tongue (green arrowheads). **B:** Photomicrograph shows the structure of the lingual papilla; connective tissue core (cc) is covered by keratinized stratified squamous epithelium (blue arrowhead), the dorsal epithelium is non-keratinized type (ED). **C:** Photomicrograph shows the transformation of epithelium from keratinized type (blue arrowhead) to non-keratinized type (red arrowhead), epithelial pegs (stars) and connective tissue papillae (arrows) at the dorsal epithelium. **D:** Photomicrograph shows non-keratinized dorsal epithelium (ED) with PAS positive intraepithelial mucous cells (red arrows). **E:** Photomicrograph shows epithelium with spiny projections (curved arrow). **F:** Photomicrograph shows the caudal end of entoglossum as a one unite (En), and it is surrounded by perichondrium (pc). Sections (A-F) were stained with H&E stain, but section (D) was stained with PAS reagent.

The caudal part of the lingual root (level caudal to the free ends of the giant papillae) showed three marked grooves: one median, and two paramedian grooves. The dorsal epithelium was non-keratinized stratified squamous epithelium with intraepithelial mucous glands (Fig. 9A, B). The glands reacted positively with PAS reagent (Fig. 9C). The submucosa contained the paired ceratobranchial bones, in addition to the urohyal (*os basibranchial caudalis*). All of these hyoid skeletal elements were ossified (Fig. 9D). The muscle ceratoglossus attached to the ceratobranchial bones (Fig. 9A), and the muscle terminated rostrally at the ventral surface of the

entoglossum (Fig. 5F, 6A). The muscle cricohyoideus was paired muscle appearing dorsal to the urohyal (Fig. 9A), and it extended caudally to the ventrolateral surface of the paired cricoid cartilage.

The lingual glands (*linguales anteriors et posteriors*) were mucous salivary glands, located within the lingual submucosa. The submucosa of the lingual body contained anterior lingual glands, which did not extend to the lingual apex. The anterior lingual glands appeared as two separated groups lateral to the entoglossum (Fig. 5E, 6A), and the number of the glandular units was increased toward the base of the tongue. Characteristically, the anterior lingual glands were continued caudally at the lingual root as posterior lingual glands (Fig. 8E). The glandular tissue was divided into lobules by connective tissue septa (Fig. 10A). The tubuloalveolar secretory units of the glands were formed of tall columnar mucous cells that by H&E stain appeared with faintly stained, foamy and vacuolated cytoplasm, and it showed flat basally located nuclei (Fig. 10B, C). The ducts of the glands opened at the ventral epithelium of the tongue (Fig. 10D). The mucous cells showed a positive reaction to the PAS techniques (Fig. 10E, F).

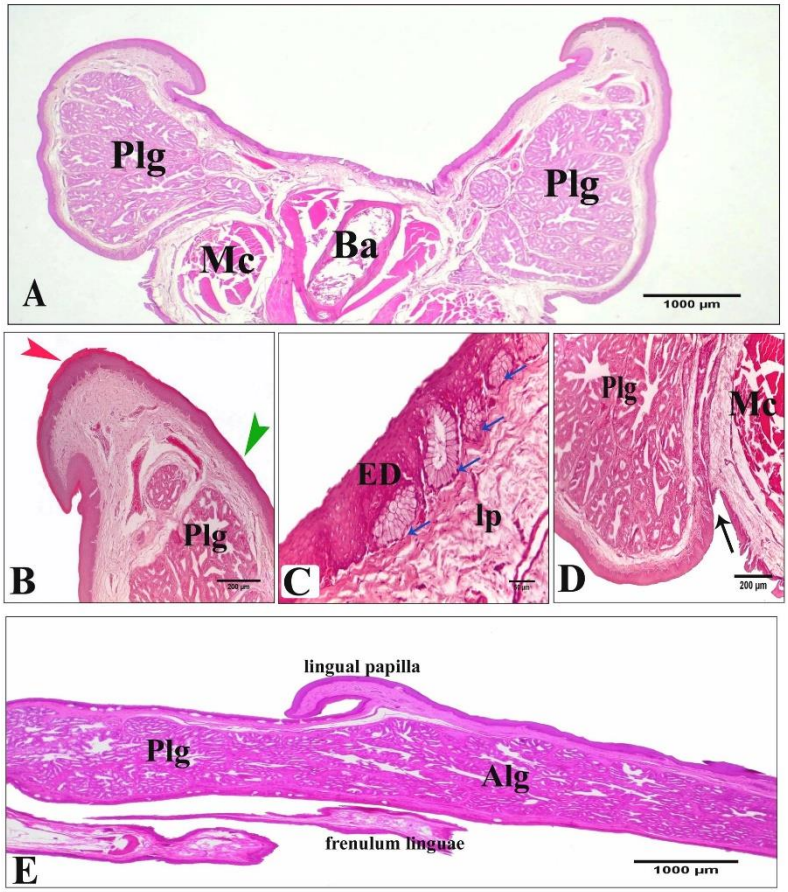

Figure (8): Histological images at the lingual root level in cattle egret. **A:** Cross section shows laterally situated posterior lingual glands within the submucosa (Plg), basiyal (Ba), and ceratoglossus muscle (Mc). **B:** Magnified image shows keratin layer covers the surface of the lingual papilla (red arrowhead) and continues on the lateral surface of the tongue (green arrowhead). **C:** Magnified image shows non-keratinized stratified squamous epithelium covers the dorsal surface (ED), with intraepithelial glands (blue arrows). **D:** Magnified image shows posterior lingual glands (Plg) open at the ventrolateral edge of the tongue (arrow). **E:** Longitudinal section shows anterior lingual gland (Alg), posterior lingual glands (Plg), lingual papilla, and frenulum linguae. All sections were stained with H&E stain.

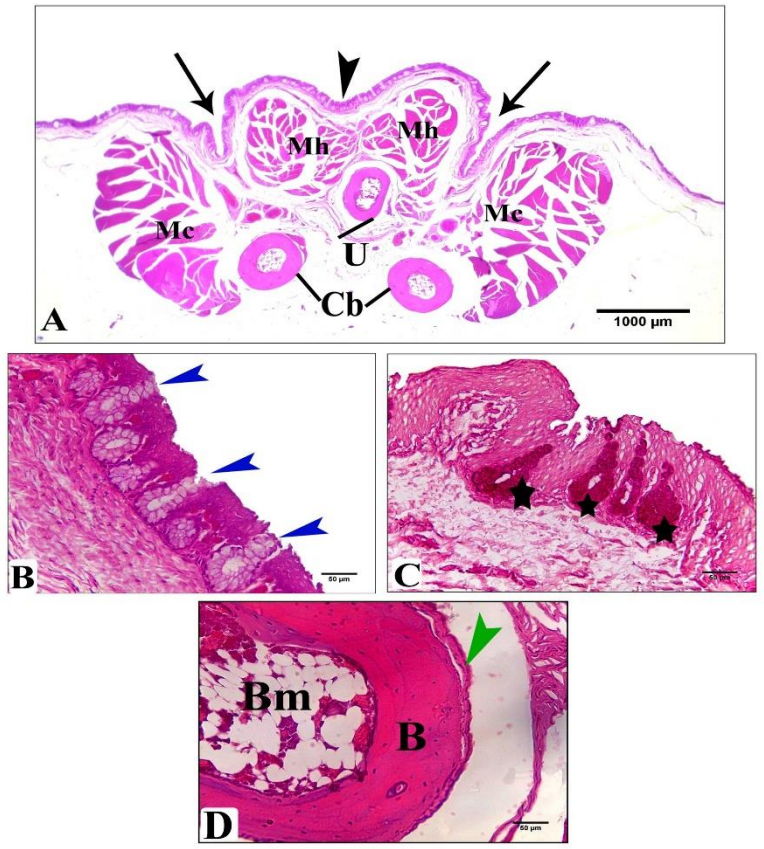

Figure (9): Histological images at the caudal part of the lingual root. **A:** Photomicrograph shows median groove (black arrowhead), two paramedian grooves (two arrows), ceratoglossus muscle (Mc) is related to ceratobranchial bone (Cb), ossified urohyal (U), and cricohyoideus muscle (Mh). **B:** Magnified photomicrograph shows intraepithelial mucous glands (blue arrowheads). **C:** Photomicrograph shows PAS positive mucous cells (stars). **D:** Photomicrograph shows the structure of ceratobranchial bone, bone tissue (B), bone marrow (Bm), and periosteum (green arrowhead). Sections (A-D) were stained with H&E stain. Section (C) was stained with PAS reagent.

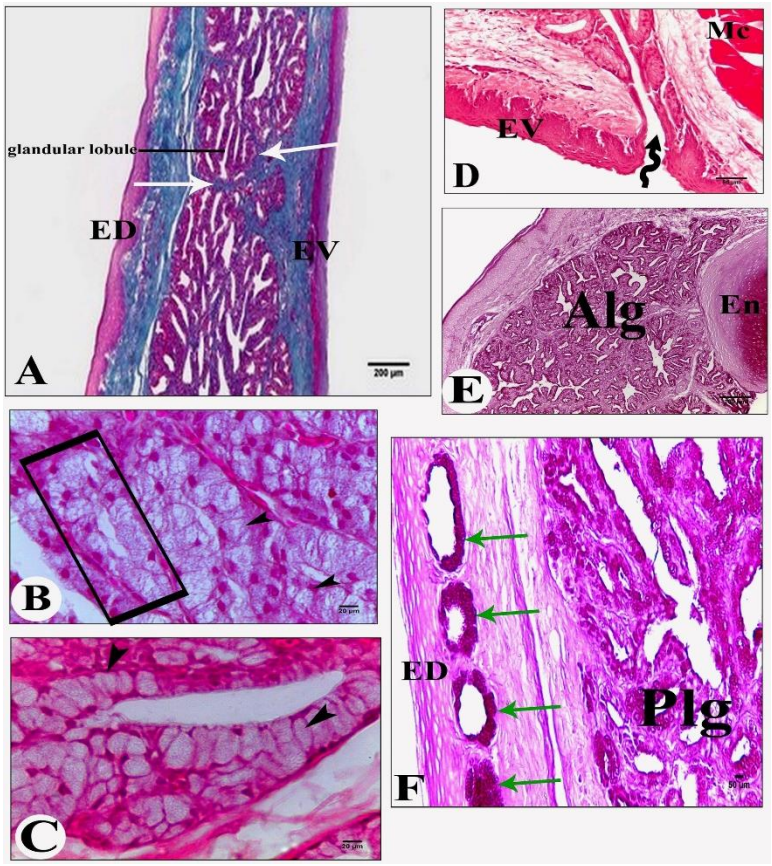

Figure (10): Histological images showing the lingual salivary glands. **A:** Longitudinal section shows the glandular tissue is divided into lobules by connective tissue septa (white arrows). **B:** Photomicrograph shows anterior lingual glands contain tubuloalveolar secretory unites (framed box) carrying mucous cells (arrowheads). **C:** Photomicrograph shows posterior lingual glands with mucous cells (arrowheads). **D:** Photomicrograph shows the opening of the duct of the anterior lingual glands (zigzag arrow) at the ventral epithelium (EV). **E:** Photomicrograph shows anterior lingual glands (Alg) with positive PAS reaction. **F:** Photomicrograph shows posterior lingual glands (Plg), and the intraepithelial mucous glands (green arrows) give strong positive PAS reaction. Section (A) was stained with Masson's trichrome stain. Sections (B-D) were stained with H&E stain. Sections (E&F) were stained with PAS reagent.

DISCUSSION

Most bird species are characterized by triangular-shaped tongues, such as the house sparrow (Abumandour, 2018), hooded crow (Gewaily and Abumandour, 2021), and broad-breasted white turkey (Madkour, 2022). The result of the current work corresponded with Abumandour et al. (2021) in the rock pigeon that the tongue is elongated organ with a pointed apex. In contrast, the tongue in the Eurasian coot is an elongated oval-in shape (Abumandour and El-Bakary, 2017a). Many other shapes of the tongue are observed in birds; Jackowiak and Ludwig (2008) described the tongue as semicircular in ostrich, it is arrowhead-shaped in the Eurasian hoopoe (Abumandour and Gewaily, 2019), it looks like a spear in zebra finch, while it is long and leafy shape in starling (Taha and Al-Duleemy, 2020). Emura et al. (2009b) noticed that a spear-like tongue is also in Japanese pygmy woodpecker that feed on insects. Needle-like tongue was observed by Emura (2009c) in the little egret, and two other heron species. The form of the tongue in the current work is closely conformed to that of the lower beak. This result in consistent with the reports in many other avian species (Abumandour and El-Bakary, 2019; Gewaily and Abumandour, 2021; Madkour, 2022). On the other hand, some birds showed tongues that are not correlated to the size of the lower beak due to the presence of very short tongues, as in ostrich, the Eurasian hoopoe and the Egyptian nightjar (Abumandour and Gewaily, 2019; El-Mansi et al., 2020; Jackowiak and Ludwig, 2008), or as a consequence of the tongue being longer than the lower beak, as it was observed in the Japanese pygmy woodpecker (Emura et al., 2009b).

Nickel et al. (1977) attributed these differences in the shapes and sizes of the tongue between the species to each bird's need to achieve its required function based on its feeding pattern. The present work is consistent with reports of Al-Ahmady Al-Zahaby (2016), in cattle egret, who recorded that, not only the shape and size of the tongue help its function, but the extremely pointed lingual tip, resampling a needle tooth, may give it a proper ability for searching for insects and earthworms in agricultural lands. To know, the apex of the tongue had a varied appearance among the bird species; it was rounded as in Garganey, the Eurasian hoopoe, the Egyptian laughing doves, and the Eurasian common moorhen (Abumandour et al., 2019; Abumandour and El-Bakary, 2019; Abumandour and Gewaily, 2019; Bassuoni et al., 2022). It appeared bifid at its anterior tip as in Hume's tawny owl (Abumandour and El-Bakary, 2017b), hooded crow (Gewaily and Abumandour, 2021), and in white-eared bulbul (Al-Khafaji and Al-Kafagy, 2024). It was spatula-shaped in Khaki Campbell duck and bronze fallow cockatiel (Al-Khafaji and Al-Kafagy, 2024; Khatun and Das, 2022). Lip-like lingual apex with many grooves characterized

the tongue in the scarlet macaw (Emura et al., 2012).

However, avian species differ slightly in the shape and number of papillary rows on their papillary crests without consideration of their feeding styles (Abumandour, 2018, Mahdy, 2021). Our finding revealed a U-shaped papillary crest between the lingual body and root; it included two large pointed conical papillae laterally (giant papillae), and in between them, there was a row of small caudally directed mechanical papillae. In general, these papillae help the function of transporting of food (regardless of its type) to the esophagus and preventing its return outside the mouth cavity (Erdoğan and Iwasaki, 2014; Gewaily and Abumandour, 2021; Mahdy, 2021). The same shape of papillary crest was observed in adult pigeon, rock pigeon, and kestrel (Abumandour and El-Bakary, 2017b; Abumandour et al., 2021; Mahdy, 2021). In many other avian species, the papillary crest is V-shaped (Abumandour, 2018; Madkour, 2018, 2022; Skieresz-Szewczyk et al., 2021). In contrast, the caudal lingual papillae are not obvious in ostrich (Jackowiak and Ludwig, 2008) or in Japanese pygmy woodpecker (Emura et al., 2009b). Anatomically, such papillae are completely absent in adult rhea (Santos et al., 2011). In contrast, KOBAYASHI et al. (1998) recorded that the absence of the transverse papillary crest in penguins, the lingual papillae are arranged longitudinally on the whole surface of the tongue. Our gross results indicated that the dorsal surface of the lingual body showed a median longitudinal sulcus which extended to a distance rostrally on the lingual apex, it was shallow and narrow groove. Controversially, by SEM, abundant ducts of the lingual salivary glands appeared only at the caudal part of this dorsal sulcus. Generally, all the studies confirmed that there was no correlation between the lingual sulcus and the different feeding patterns of the avian species (Abumandour and El-Bakary, 2019; Erdogan and Alan, 2012).

According to the SEM examinations of the present study, the dorsal surface of the anterior free part of the tongue did not carry any papillae, whereas it displayed scale-like structures that represented the exfoliation of the superficial epithelial cells. In the same regard, Abdelhakeem et al. (2025) recognized structures on the tongue, each looked like a rosette, while Mahdy (2021) noted the presence of scale-like papillae in adult pigeon that were absent on the median lingual sulcus, as well as the scale-like filiform papillae that were observed in rock pigeon (Abumandour et al., 2021). Characteristically, our SEM study revealed numerous longitudinal microgrooves of varying lengths on the dorsum of the tongue's anterior part, marked by longitudinal microridges. While, lingual root was dorsally perforated by openings of lingual salivary gland, these openings increased in number caudal wards. A similar finding is recorded by Mahdy (2021) in pigeon; however, the same author noted that the

openings of the glands were at the apex of lingual projections. On the other hand, in some insectivorous birds such as bobwhite, the dorsolateral parts of its lingual apex and body featured hair-like and rosette-shaped filiform papillae that varied in density and size (Madkour et al., 2025).

With the help of stereomicroscopy, this work recorded the presence of a median longitudinal ridge on the ventral surface of the tongue. This bulged region was due to the presence of the entoglossum and its related muscle bundle that appeared by using SEM at the midsagittal section of the tongue. The ventral surface of the tongue in this study was attached to the floor of the oropharynx by a thin mucosal fold (lingual frenulum). Attention should be paid to the level of attachment of this fold to the tongue, in this work the lingual frenulum was attached to the tongue at the level of the papillary crest; thus, the anterior free part of the tongue was markedly long and freely movable. Similar findings were in pigeon and the Eurasian coot (Abumandour and El-Bakary, 2017a; Mahdy, 2021). In bulbul, the fold is attached at the level of the middle part of the lingual body, however in cockatiel, it attached at the beginning of the lingual body (Al-Khafaji and Al-Kafagy, 2024). Rodrigues et al. (2012) observed the absence of the distinct lingual frenulum in rhea and the presence of numerous mucosal folds.

Our histological findings revealed that thick keratinized stratified squamous epithelium lined the dorsal aspect of the tongue, except for the caudal part of the lingual body and the lingual root. Ozkadif et al. (2023) noted the reverse in barn owl; non-keratinized epithelium covers the dorsal surface of the tongue, which is keratinized epithelium at its caudal part. El-Badry (2022) recorded the complete absence of keratinization on the lingual body and root of C. coturnix. In general, the type of epithelia of the tongue in birds is affected by the dietary habits of each species; either it is keratinized or non-keratinized stratified squamous epithelium (Al-Kafagy et al., 2022). The epithelia of tongues of most predatory birds are non-keratinized (Abumandour and El-Bakary, 2017b). On the contrary, the common epithelium of the tongue of herbivorous birds is keratinized (Iwasaki, 1992). Additionally, our investigation clarified that the ventral epithelium of the tongue showed a variety in the degree of keratinization. Caudal to the lingual tip, the thick keratin layer organized on the ventral ridge and its thickness decreased on the other parts of the ventral surface. However, gradually the ventral epithelium transformed into non-keratinized type at the caudal part of the tongue. On the contrary, keratinized epithelium covers the whole ventral surface of the tongue in barn owl (Ozkadif et al., 2023).

Our histological results revealed that the tongue tip consisted of a collagenous connective tissue core covered by a thick, highly organized keratin layer. Abumandour and Gewaily (2019)

noted that the keratinized stratified squamous epithelium lining the tongue in the Eurasian hoopoe adapts to food manipulation. In the hooded crow, the anterior lingual tip has a keratin layer forming a lingual nail (Gewaily and Abumandour, 2021). Histological sections in the tongue clarified the presence of the elements of the hyoid bone in the submucosa of the tongue; the entoglossum extended from the lingual apex to the level of the papillary crest of the tongue. Similar observation was recorded by Abumandour and El-Bakary (2017b) in the tongue of the common kestrel and Hume's tawny owl. In herons, the entoglossum extends to the lingual apex to adapt the tongue with the long beak (Homberger, 2017). Additionally, our investigation recorded at the first time the fusion of the two caudal processes of the entoglossum, while the previous study by Al-Ahmady Al-Zahaby (2016) in cattle egret stated that the body of entoglossum extends to the lingual root, where it bifurcates into two roots of entoglossum. To know, Crole and Soley (2012) reported that the entoglossum in Rhea Americana shows an oval opening but of undefined function. The current work revealed the entoglossum was a hyaline cartilaginous plate along its length. Whereas, the entoglossum in ducks and geese is cartilaginous at the rostral part of the tongue and it is ossified toward the lingual root (Alzebari and Alhasso, 2023).

The lingual root in this study was supported by an ossified basihyal which extended rostrally to support the lingual body where it was a hyaline cartilaginous skeleton. The basihyal articulated rostarally with the entoglossum this articulation provided the lingual body the ability to move up and down as well as slightly from side to side (Homberger, 2017). Additionally, the present work could detect an ossified urohyal that supported the caudal part of the tongue and extended ventrally to the laryngeal mound, as well as the paired bony ceratobranchial that articulated with the basibranchial at the basihyal-urohyal transition. Different degrees of ossification of the hyoid elements may raise the efficiency of the mechanical performance of the tongue (Mahmoud et al., 2019). The current work investigated intra-lingual parts of extrinsic skeletal muscles in the tongue via the histological sections. Gewaily and Abumandour (2021) suggested that the intra-lingual skeletal muscles help the function of the tongue through controlling its active protrusion and movement. Corresponding to Huang et al. (1999), M. ceratoglossus is one of the lingual muscles, it is paired muscle that originates from the ceratobranchial bone and inserts on the ventral surface of the entoglossum. Additionally, M. cricohyoideus is an infrahyoid muscle, a paired muscle laying close to the midline, it originates from the cricoid cartilages of the larynx and inserts dorsal to basibranchial bone. Contraction of this muscle retracts the hyoid elements.

Our findings in the current work noted that well-developed glandular tissue was in the

submucosa of the tongue, and all glands were mucous type. In agreement with Homberger (2017), who reported that insectivorous birds have numerous salivary glands of mucous type, which is the predominant type in birds in general. The development of these glands shows variations between the avian species, and they are completely absent in cormorant birds (Sturkie, 2000). And also, Rab et al. (2017) stated that the lingual glands are not evident in the common hoopoe and the author explained this absence due to the small-sized free lingual part and the soft food intake. According to Hodges (1974) the lingual glands are classified in chickens according to their location in the tongue into anterior (in the lingual body) and posterior (in the lingual root) lingual glands. However, the glands in quail are divided into lingual and preglottal glands (Liman et al., 2001). The present study agrees with Al-Ahmady Al-Zahaby (2016) that in cattle egret, anterior lingual glands at the lingual body are two separate right and left groups that continue uninterrupted into the lingual root as posterior glands. However, this study disagrees with the latter author on the glands in the submucosa extending to the rostral edge of the laryngeal mound. Our findings showed these glands were absent in the preglottal area, with only intraepithelial mucous glands present. Compound tubuloalveolar glands within the lingual tissue were recorded in this work, similar observations were recorded by Dehkordi et al. (2010) in zebra finch.

The present study is in agreement with reports of Rab et al. (2017), who found that the lingual glands are separated into lobules by collagenous connective tissue septa. The latter authors added that each glandular group may be surrounded by connective tissue envelope that give the tongue an additional skeletal support. With Periodic Acid–Schiff stain the glands in cattle egret reacted positively by giving a strong magenta color, therefore it demonstrates the presence of neutral mucopolysaccharides which were secreted by the cells of these glands, similar findings could be detected in the common kestrel, Hume's tawny owl, and laughing dove (Abumandour and El-Bakary, 2017b; Rab et al., 2017). Functionally, the mucous secretions of the salivary glands lubricate the food in the oropharyngeal cavity and help its passage to the esophagus (Rab et al., 2017).

After studying the feeding style of cattle egret, we could conclude that the lingual tip is used during the food selection, thus it is very thin to work efficiently, and it is wholly wrapped with a circumscribed thick keratin layer for protection (the lingual nail). This lingual nail continued on the ventrum of the anterior part of the lingual body giving the tongue an additional support where it is considered as an exoskeleton, also its bending ability facilitated the picking up of the selected food as well as the drinking process (Crole and Soley, 2010b; Rab et al., 2017). To

conduct the food items to the esophagus, the food must pass along the dorsal surface of the tongue; therefore, the tongue has a visible dorsal longitudinal sulcus to control this process. Moreover, the tongue characteristically shows several microgrooves that may prevent food slippery. Consequently, at the pharynx, the food is caudally directed by the aid of the papillary crest and the sticky mucous of the numerous glands at the lingual root (Zweers et al., 1994). As for the lingual free part, the mucous secretion of the lingual glands in the submucosa are evacuated via their ducts to the ventral surface of the tongue at the caudal half of the lingual body where the lining epithelium was non-keratinized type, conversely, the openings of these ducts are not evident to a large extent dorsally in which the lining epithelium was significantly keratinized type. The latter features strongly clarify the special epithelial modifications in the tongue to be correlated with its function in general.

CONCLUSION

The authors concluded that, the anatomical form of the tongue of cattle egret is closely related to the form of the lower beak. The ultrastructural composition of the lingual dorsal surface by light and scanning electron microscopy showed characteristic features in the examined birds. Moreover, the illustrated histological specifications of the lingual apparatus in this work reflect the adaptation of this organ to the feeding pattern.

ACKNOWLEDGMENT

The authors would like to express their sincere thanks to the staff of the department of Anatomy and Embryology, Faculty of Veterinary Medicine, South Valley University, Qena, Egypt, for their help and cooperation that greatly facilitated the progress of this work.

CONFLICT OF INTEREST

The authors declare that there is no conflict of interest exist.

REFERENCES

Abdelhakeem F, Mohamed SA, Abdelsabour-Khalaf M, Soliman S and Abdalla KE (2025). Functional morphological study on the tongue of the adult Egyptian geese (Alopochen egyptiacus). BMC Veterinary Research, 21, 1-17.

Abdellatif AM, Lashen S, Kandyel RM, Shoeib MB and Madkour FA (2024). Age-related morphological and ultrastructural changes in the palate and pharyngeal masticatory apparatus of grass carp (Ctenopharyngodon idella) juveniles. Tissue and Cell, 86, 102264.

Abumandour M and El-Bakary N (2017a). Morphological characteristics of the oropharyngeal cavity (tongue, palate and laryngeal entrance) in the Eurasian coot (Fulica atra, Linnaeus, 1758). Anatomia, histologia, embryologia, 46, 347-358.

Abumandour MM (2018). Surface ultrastructural (SEM) characteristics of oropharyngeal cavity of house sparrow

(Passer domesticus). Anatomical science international, 93, 384-393.

Abumandour MM, Bassuoni NF and Hanafy BG (2019).Surface ultrastructural descriptions of the oropharyngeal cavity of Anas querquedula. Microscopy Research and Technique, 82, 1359-1371.

Abumandour MM and El-Bakary NE (2017b). Morphological features of the tongue and laryngeal entrance in two predatory birds with similar feeding preferences: common kestrel (Falco tinnunculus) and Hume's tawny owl (Strix butleri). Anatomical Science International, 92, 352-363.

Abumandour MM and El-Bakary NE (2019). Anatomical investigations of the tongue and laryngeal entrance of the Egyptian laughing dove Spilopelia senegalensis aegyptiaca in Egypt. Anatomical Science International, 94, 67-74.

Abumandour MM, El-Bakary NE, Elbealy ER, El-Kott A, Morsy K, Haddad SS and Kandyel RM (2021). Ultrastructural and histological descriptions of the oropharyngeal cavity of the rock pigeon Columba livia dakhlae with special refer to its adaptive dietary adaptations. Microscopy research and technique, 84, 3116-3127.

Abumandour MM and Gewaily MS (2019). Gross morphological and ultrastructural characterization of the oropharyngeal cavity of the Eurasian hoopoe captured from Egypt. Anatomical science international, 94, 172-179.

Ahmed R (2011). Subspecific identification and status of Cattle Egret. Dutch Birding, 33, 294-304.

Al-Kafagy SM, Al-Jebori AK and Alseady YY (2022). Histochemical study of proventriculus in pre-hatch and post-hatch days in northern bobwhite quail (Colinus virginianus).

Al-Khafaji S and Al-Kafagy S (2024). Histological and histochemical comparative study of the tongue in white-eared bulbul (Pycnonotus leucotis) and bronze fallow cockatiel (Nymphicus hollandicus). J. Anim. Health Prod, 12, 319-325.

Al-Ahmady Al-Zahaby S (2016). Light and scanning electron microscopic features of the tongue in cattle egret. Microscopy Research and Technique, 79, 595-603.

Alzebari BS and Alhasso AA (2023). A Comparative Histological & Histochemical Study of the Tongue between the Local Adult Ducks & Geese.

Bancroft JD and Gamble M (2002). Theory and practice of histological techniques. 5th. Edinburgh. Churchill Livingstone Pub, 172, 593-620.

Bassuoni NF, Abumandour MM, Morsy K and Hanafy BG (2022). Ultrastructural adaptation of the oropharyngeal cavity of the Eurasian common moorhen (Gallinula chloropus chloropus): Specific adaptive

dietary implications. Microscopy Research and Technique, 85, 1915-1925.

Baumel, J. J., 1993. Handbook of avian anatomy: nomina anatomica avium., Publications of the Nuttall Ornithological Club (USA).

Bonaparte CL (1855). "[untitled]". Annales des Sciences Naturelles comprenant la zoologie (in French), 4, 141.

Crole M and Soley J (2010b). Surface morphology of the emu (Dromaius novaehollandiae) tongue. Anatomia, Histologia, Embryologia, 39, 355-365.

Crole M and Soley J (2012). Gross anatomical features of the tongue, lingual skeleton and laryngeal mound of Rhea americana (Palaeognathae, Aves): morpho-functional considerations. Zoomorphology, 131, 265-273.

Dehkordi RAF, Parchami A and Bahadoran S (2010). Light and scanning electron microscopic study of the tongue in the zebra finch Carduelis carduelis (Aves: Passeriformes: Fringillidae). Slov Vet Res, 47, 139-44.

El-Badry DA (2022).Comparative Histological and ultra structural Studies on the Tongue of Gallinula cholorpus and Coturnix coturnix. Journal of Environmental Sciences. Mansoura University, 51, 1-9.

El-Mansi A, Al-Kahtani M, Abumandour M, Ezzat A and El-Badry D (2020). Gross anatomical and ultrastructural characterization of the oropharyngeal cavity of the Egyptian nightjar Caprimulgus aegyptius: Functional dietary implications. Ornithological Science, 19, 145-158.

Emura S (2009c). SEM studies on the lingual dorsal surfaces in three species of herons. Medicine and Biology 2009c, 153, 423-430.

Emura S, Okumura T and Chen H (2009b). Scanning electron microscopic study of the tongue in the Japanese pygmy woodpecker (Dendrocopos kizuki). Okajimas folia anatomica Japonica, 86, 31-35.

Emura S, Okumura T and Chen H (2012). Scanning electron microscopic study on the tongue in the scarlet macaw (Ara macao). Okajimas Folia Anatomica Japonica, 89, 57-60.

Erdogan S and Alan A (2012). Gross anatomical and scanning electron microscopic studies of the oropharyngeal cavity in the European magpie (Pica pica) and the common raven (Corvus corax). Microscopy research and technique, 75, 379-387.

Erdoğan S and Iwasaki SI (2014). Function-related morphological characteristics and specialized structures of the avian tongue. Annals of Anatomy-Anatomischer Anzeiger, 196, 75-87.

Gewaily MS and Abumandour MM (2021). Gross morphological, histological and scanning electron specifications of the oropharyngeal cavity of the hooded crow

(Corvus cornix pallescens). Anatomia, histologia, embryologia, 50, 72-83.

Hodges, R. D. 1974. The histology of the fowl.

Homberger DG (2017). The avian lingual and laryngeal apparatus within the context of the head and jaw apparatus, with comparisons to the mammalian condition: functional morphology and biomechanics of evaporative cooling, feeding, drinking, and vocalization. The biology of the avian respiratory system: evolution, development, structure and function, 27-97.

Homberger DG and Meyers RA (1989). Morphology of the lingual apparatus of the domestic chicken, Gallus gallus, with special attention to the structure of the fasciae. American Journal of Anatomy, 186, 217-257.

Huang R, Zhi Q, Izpisua-Belmonte JC, Christ B and Patel K (1999). Origin and development of the avian tongue muscles. Anatomy and embryology, 200, 137-152.

Iwasaki SI (1992). Fine structure of the dorsal lingual epithelium of the little tern, Sterna albifrons Pallas (Aves, Lari). Journal of Morphology, 212, 13-26.

Jackowiak H and Ludwig M (2008). Light and scanning electron microscopic study of the structure of the ostrich (Strutio camelus) tongue. Zoological Science, 25, 188-194.

Khatun P and Das SK (2022). Gross Anatomical Features of Tongue of Khaki Campbell Duck (Anas platyrhynchos domesticus) At Different Postnatal Ages. Ukrainian journal of veterinary and agricultural sciences, 5, 17-23.

Kobayashi K, Kumakura M, Yoshimura K, Inatomi M and Asami T (1998). Fine structure of the tongue and lingual papillae of the penguin. Archives of histology and cytology, 61, 37-46.

Liman N, Bayram G and Kocak M (2001). Histological and histochemical studies on the lingual, preglottal and laryngeal salivary glands of the Japanese quail (Coturnix coturnix japonica) at the post-hatching period. Anatomia, Histologia, Embryologia, 30, 367-373.

Linnaeus, C. 1758. Systema naturae per regna tria naturae, secundum classes, ordines, genera, species, cum characteribus, differentiis, synonymis, locis, Tomus I. Editio decima, reformata (in Latin), Holmiae [Stockholm]: Laurentii Salvii.

Madkour F (2018). Characteristic features of the pharyngeal cavity of the laughing dove (Streptopelia senegalensis aegyptiaca) and Japanese quail (Coturnix coturnix). Assiut Veterinary Medical Journal, 64, 52-59.

Madkour F (2022). Beak, Oropharyngeal and nasal cavities of broad breasted white Turkey (Meleagris gallopavo): gross anatomical and Morphometrical study. Journal of Advanced Veterinary Research, 12, 99-106.

Madkour FA (2020). Comparative histology and micrometric analysis of pharyngeal cavity in Egyptian laughing dove (Streptopelia senegalensis aegyptiaca) and Japanese quail (Coturnix coturnix japonicum). SVU-International Journal of Veterinary Sciences, 3, 115-129.

Madkour FA (2024). Unique insights into morphological characterization and functional adaptation of the scaly shank skin in aquatic and terrestrial birds. Scientific Reports, 14, 28101.

Madkour FA, Abdellatif AM, Osman YA and Kandyel RM (2023). Histological and ultrastructural characterization of the dorso-ventral skin of the juvenile and the adult starry puffer fish (Arothron stellatus, Anonymous 1798). BMC veterinary research, 19, 221.

Madkour FA and Abdelsabour-Khalaf M (2022). Morphological and ultrastructural features of the laryngeal mound of Egyptian Cattle Egret (Bubulcus ibis, Linnaeus, 1758). BMC zoology, 7, 44.

Madkour FA, Hiramatsu K and Mohamed AA (2025). Scanning Electron Microscopy of the Oropharyngeal Floor of Northern Bobwhite (Colinus virginianus, Linnaeus, 1758) Focusing on the Numerical and Regional Distribution of the Taste Buds. Microscopy Research and Technique, 88, 732-748.

Mahdy MA (2021). Comparative morphological study of the oropharyngeal floor of squabs and adult domestic pigeons (Columba livia domestica). Microscopy Research and Technique, 84, 499-511.

Mahmoud FA, Gadel-Rab AG, Saber SA, ElSalkh BA, El-Dahshan AA and Gewily DI (2019). Comparative anatomical study of the hyoid apparatus of Bosk's fringe-toed lizard and spotted fan-toed gecko (Squamata: Lacertidae and Phyllodactylidae). The Journal of Basic and Applied Zoology, 80, 1-8.

McAllan I, Bruce MD, Atlassers NSWB and Group BR (1988). The birds of New South Wales: a working list, Biocon Research Group in association with the New South Wales Bird Atlassers.

McKilligan, N. 2005. Herons, egrets and bitterns: Their biology and conservation in Australia, CSIRO publishing.

Moussa, M. S., 2014. A dictionary of idiomatic expressions in written Arabic: for the reader of classical and modern texts, American University in Cairo Press.

Mullarney, Svensson, K., Zetterström, L., Grant and J.P, 2001. Birds of Europe. Princeton University Press.

Nickel, R., Schummer, A. and Seiferle, E., 1977. Anatomy of the domestic birds.

Ozkadif S, Haligur A, Haligur M and Alan A (2023). Morphological examination and scanning electron microscopy of the barn

owl's (Tyto alba) tongue. Microscopy Research and Technique, 86, 747-753.

Rab AGG, Shawki NA and Saber SA (2017). Morpho-functional adaptations of the lingual epithelium of two bird species which have different feeding habits. The Egyptian Journal of Hospital Medicine, 69, 2115-2127.

Rodrigues MN, Tivane CN, Carvalho RC, Oliveira GB, Silva RS, Ambrosio CE and Miglino MA (2012). Gross morphology of rhea oropharyngeal cavity. Pesquisa Veterinária Brasileira, 32, 53-59.

Santos TC, Fukuda KY, Guimarães JP, Oliveira MF and Miglino MA (2011). Light and scanning electron microcopy study of the tongue in Rhea americana. Zoological Science, 28, 41-46.

Skieresz-Szewczyk K, Plewa B and Jackowiak H (2021). Functional morphology of the tongue in the domestic turkey (Meleagris gallopavo gallopavo var. domesticus). Poultry science, 100, 101038.

Soliman SA and Madkour FA (2017). A comparative analysis of the organization of the sensory units in the beak of duck and quail. Histol Cytol Embryol, 1, 1-16.

Sturkie P., 2000. Sturkie's Avian Physiology-/ed. by G. Causey Whittow, Academic Press.

Taha AM and & Al-Duleemy AS (2020).Morphological description of the digestive canal in Taeniopygia guttata (zebra finch) and Sturnus vulgaris (starling). The Journal of Basic and Applied Zoology, 81, 1-10.

Zweers GA, Berkhoudt H and Vanden Berge JC (1994). Behavioral Mechanisms of Avian Feeding. In: BELS, V. L., CHARDON, M. & VANDEWALLE, P. (eds.) Biomechanics of Feeding in Vertebrates. Berlin, Heidelberg: Springer Berlin Heidelberg.